J. Am. Ceram. Soc., **94** [11] 4084–4088 (2011)
DOI: 10.1111/j.1551-2916.2011.04704.x

Journal

Growth of Al_2O_3 Nanowires on the Cu-9 at.%Al(111) Single Crystal Surface

Iva Matolínová,[‡,†] Slavomír Nemšák,[§] Miloš Cabala,[‡] Nataliya Tsud,[‡] Jana Poltierová-Vejpravová,[¶]
Kateřina Veltruská,[‡] Michiko Yoshitake,[§] and Vladimír Matolín[‡]

[‡]Department of Surface and Plasma Science, Faculty of Mathematics and Physics, Charles University in Prague,
18000, Prague, Czech Republic

[§]Advanced Electronic Materials Center, National Institute for Materials Science,
Tsukuba, Ibaraki, 305-0003, Japan

[¶]Department of Condensed Matter Physics, Faculty of Mathematics and Physics, Charles University in Prague,
12116, Prague, Czech Republic

Aluminum oxide structures were grown on Cu–9 at.%Al(111) single crystals. Usually alumina grows in the form of an epitaxial thin film. The process is based on Al atom segregation and subsequent oxidation of the Al topmost surface. Strong temperature dependence of the alumina growth mode was observed during the oxidation of a Cu–9 at.%Al single crystal. In this work we have reported for the first time the formation of alumina wire-like nanostructures on the substrate surface during high-temperature oxidation at low pressure. The nanowire growth was observed during substrate annealing at 1070 K while annealing at 910 K led to the formation of a flat and continuous thin alumina layer. Morphology, chemical composition, and structure characterization of the prepared nanostructures was done by means of scanning electron microscopy, energy-dispersive X-ray spectroscopy, X-ray photoelectron spectroscopy, and X-ray diffraction. The experimental results point to the formation of Θ alumina phase nanowires due to surface segregation of Al atoms. Mechanism of alumina nanostructure formation is discussed. The experiment clearly showed that nanowire oxide structure growth can be obtained by a bottom-up process with a mass transfer from the substrate to the assembled nanostructure.

I. Introduction

Aluminum oxide has been extensively studied in recent years due to its wide potential of applications in electronics, catalysis, sensors, fuel cells, and data storage devices.[1–3] Since the beginning of the electronic industry, the trend of reducing the size, cost, and power consumption is permanently present, and nanostructured alumina has therefore attracted much attention. Recently, alumina nanostructures have been prepared by various methods, e.g. by chemical etching of highly ordered porous anodic aluminum oxide membranes,[4–6] by calcination of nanocrystalline boehmite (AlOOH) or pseudo boehmite synthesized by sol–gel, hydrothermal or solvothermal methods.[7,8] Gan *et al.*[9] synthesized mezoporous alumina nanostructures with tunable morphologies through the template-free solvothermal approach. Liu *et al.*[10] applied chemical precipitation method to prepare γ-Al_2O_3 nanofibers. Alumina nanoribbons and nanorings were prepared via high temperature route using aluminum foil and SiO as a precursor.[11]

Several groups have been interested in the formation of alumina during high temperature oxidation processes of alumina-forming alloys.[12–14] Studies of thin alumina film growth and structures[13–15] have pointed to the formation of γ- and θ-Al_2O_3 layers on NiAl(001) and NiAl(110) single crystals. By oxidizing NiAl surfaces vicinal to the (100) plane tilted along crystallographic direction [010], Luo *et al.*[16] have prepared θ-Al_2O_3 strips along [001] direction. The formation of the ultra-thin well-ordered stoichiometric γ-Al_2O_3 layer on the Cu–9 at.%Al(111) single crystal was reported with an optimal oxidation procedure by Yoshitake *et al.*[14,17–19]. By dosing of oxygen at 910 K the well-ordered γ-Al_2O_3 film of $(7/\sqrt{3} \times 7/\sqrt{3})R30°$ structure and thickness up to 3–4 nm has been obtained. A thin alumina film grown by Varga *et al.*[20] exhibited a different structure due to lower preparation temperature.

In this article, we report strong structural dependence of alumina growth on Cu–9 at.%Al(111) on oxygen exposure and temperature. For the first time we show the low pressure growth of alumina nanowires based on aluminum diffusion from the substrate.

II. Experimental Procedure

A Cu–9 at.%Al(111) single crystal was introduced into the chamber equipped with an X-ray photoelectron spectroscopy subsystem (XPS). The sample was first cleaned by cycles of Ar^+ sputtering at room temperature and annealing at 770 K until no trace of impurity was detected.[17] Then the sample was oxidized at different temperatures under a partial oxygen pressure of 8×10^{-6} Pa.

Chemical composition and cleanness of the sample surface was checked by XPS. XPS measurements were performed with a conventional X-ray source using the Al*K*α line ($h\nu = 1486.6$ eV) and a multichannel energy analyzer (SPECS Phoibos MDC 9) at a total resolution $\Delta E = 1$ eV. All XPS experiments were performed *in situ* in an ultra-high vacuum experimental chamber operating at base pressures $< 10^{-8}$ Pa.

Surface morphology was observed *ex-situ* by means of scanning electron microscopy (SEM, TESCAN – MIRA) at electron beam energy of 15–30 keV. The microscope was equipped with a detector for energy dispersive X-ray spectroscopy (EDX, Bruker XFlash 4010).

For structure characterization the X-ray diffraction (XRD) patterns were recorded on a diffractometer (X'pert Pro Material Research Diffractometer) using monochromatized Cu*K*α source ($\lambda = 1.54056$ Å) at 3° incidence angle.

W. Mullins—contributing editor

Manuscript No. 28607. Received September 14, 2010; approved May 20, 2011.
This work was supported by the Ministry of Education of the Czech Republic, under the Research Programs No. MSM 0021620834 and No. LC08056, and by the Czech Grant Agency, under Grant No. 202-09-H041.

[†]Author to whom correspondence should be addressed. e-mail: imatol@mbox.troja.mff.cuni.cz

III. Results and Discussion

Annealing of the Cu–9 at.%Al(111) single crystal in oxygen atmosphere at 910 K leads to the formation of a continuous single-crystalline alumina thin film.[14,17–19] In Fig. 1 we present the result of such process after 9 h and 16 min of annealing corresponding to a total oxygen exposure of 2000 L. SEM image shows residual holes in the alumina film. It points out that the oxidation process was stopped before the completion of the alumina film which is grown in Frank–Van der Merwe mode.[21] Hexagonal symmetry of hole borders, highlighted with bright edges in Fig. 1 due to the edge effect (more secondary electrons escape from areas with sharp edges than from flat ones),[22] reflects the hexagonal symmetry of the substrate. Holey character of hexagonal structures was confirmed by SEM observations of hole borders at higher magnifications (not shown).

By increasing the annealing temperature we obtained completely different mode of aluminum oxide growth characterized by the formation of nanowires. After heating of the Cu–9 at.%Al(111) single crystal at 1070 K for 18 h 30 min (i.e. oxygen exposure of 4000 L at 8×10^{-6} Pa) the surface was covered by wire-like structures as can be seen in Fig. 2. A detailed view of typical nanowires presented in Fig. 3 reveals a predominantly bent shape; the wires are 2–5 μm long and 50–200 nm thick. However, some parts of the sample exhibit well-shaped straight whisker-like structures, as can be seen in Fig. 4(a), suggesting single-crystalline growth. It seems that this is due to overheating of these parts of the Cu–9 at.%Al(111) single crystal. Figure 5 presents a side view showing wire bases. The nanowires are ended with thicker termination at the Cu–9 at.%Al alloy substrate that was observed for most the structures.

The chemical analysis was done by performing EDX that provided a quantitative estimation of the concentration ratios of elements present in the sample. X-ray emission spectra were analyzed after subtracting a contribution from the bremsstrahlung background. Spectra were recorded at three points, at the wire base (point 1), at the central part, (point 2) and at the Cu–Al alloy surface out of the nanostructures (point 3), as can be seen in Fig. 3. Results of EDX point analysis are summarized in Table I. One can see that the nanostructure contains higher concentration of aluminum and oxygen than the substrate; the highest content of aluminum was detected at the wire root. The EDX element map of the bottom part of the crystalline nanowire [Fig. 4(a)] presented in Fig. 4(b) confirms the distribution of Cu, Al, and O atoms. Therefore, we consider the nanostructures to be composed of aluminum oxide.

Chemical composition of the sample was further investigated by XPS. The O 1*s* spectrum of the oxidized Cu–9 at.% Al(111) sample with nanostructures on the surface marked "nanowires" is shown in Fig. 6(a). For comparison, we added the O 1*s* spectrum acquired from the reference oxide layer presented in Fig. 1. The O 1*s* reference peak intensity was ~10 times higher and, for better clarity, we divided its intensity in Fig. 6(a) by a factor of 10. The spectrum (see dashed line) is characterized by a peak at 532.3 eV corresponding to oxygen from aluminum oxide.[23] Because of small thickness of the oxide film, no charging effect was observed. The O 1*s* spectrum of the sample with nanowires is composed of two components. The main O 1*s* peak appears at an unusually high binding energy of 536.1 eV, which can be explained by O 1*s* photoemission from charged alumina (by 3.8 eV) due to worse charge transfer to the substrate. The photoemission intensity at 532.1 eV corresponds to charge-free aluminum oxide ultra-thin film covering the

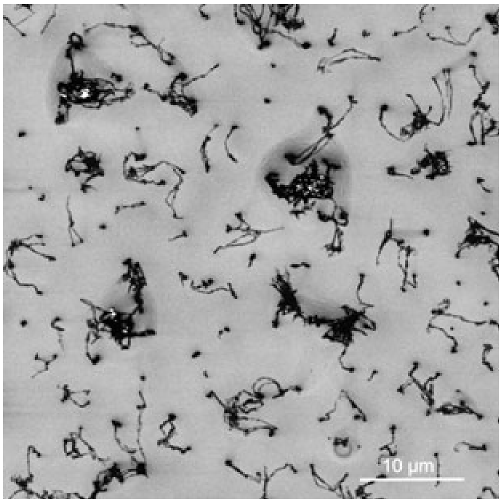

Fig. 2. SEM image of the Cu–9 at.%Al(111) surface covered by alumina nanowires. The image was acquired in combination with backscattered-electron (BSE) and secondary-electron modes (SE) to obtain atomic-number contrast together with topographical contrast and shadowing effects.

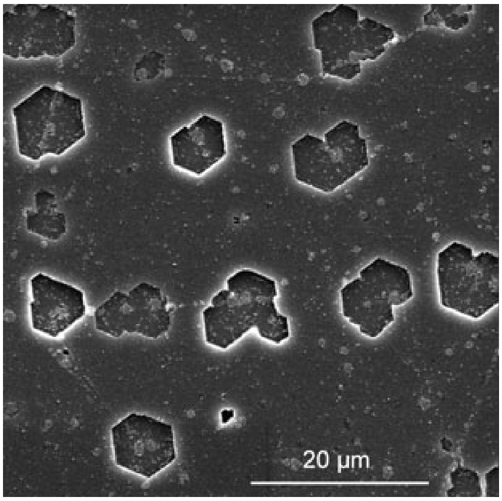

Fig. 1. SEM image of the holey structure of the alumina film grown on Cu–9 at.%Al(111). To display topographical contrast the secondary-electron image was acquired. It results in appearing as a bright outline of the holes due to the edge effect.

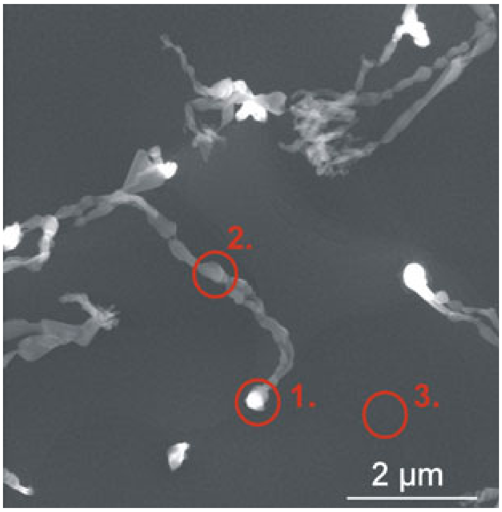

Fig. 3. Detailed view of alumina nanowires. The image was acquired in secondary-electron mode (SE). In centers of the marked red circles EDX point analysis was done, the results are presented in Table I.

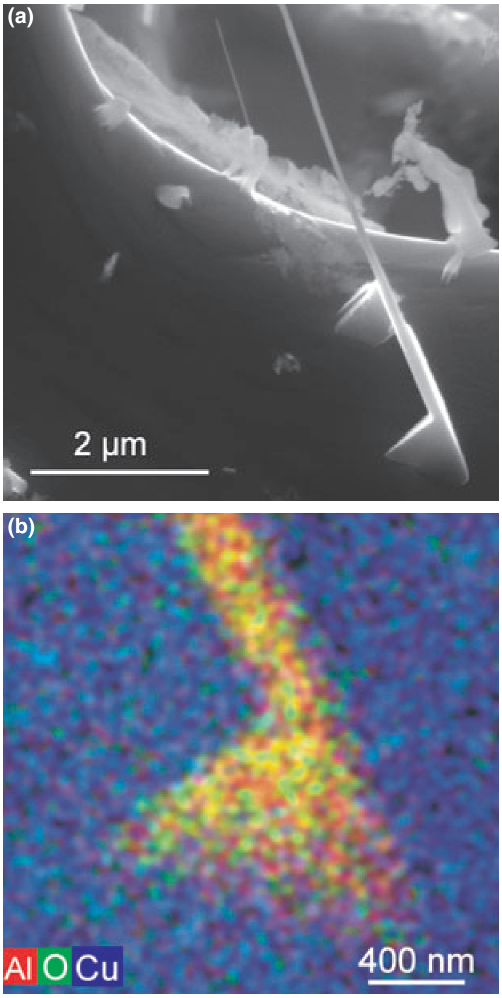

Fig. 4. Secondary-electron image of well-shaped straight whisker-like structures (a). EDX element map of the bottom part of the structure showing distribution of Al, O, and Cu atoms (b).

Table I. EDX Point Analysis from Points Indicated in Fig. 3

Point	Cu (at.%)	Al (at.%)	O (at.%)
1	43.8	20.2	36.0
2	54.4	14.9	30.7
3	67.0	8.2	24.8

substrate crystal surface similar to the case of the reference oxide layer. It showed clearly that higher oxidation temperature did not lead to a continuous oxide formation because O 1*s* intensity of the non-shifted peak was smaller by two orders of magnitude relative to the reference sample.

In Fig. 6(b) we compared the Cu 3*p* + Al 2*p* spectra of the clean non-oxidized substrate (bottom spectrum) and the oxidized samples-the surface covered by the nanowires (middle spectrum) and the reference alumina layer (upper spectrum). Main peaks at 75.2 and 77.6 eV in Fig. 6(b) correspond to Cu $3p_{3/2}$ and Cu $3p_{1/2}$ photoemission. Shoulder at 72.9 eV corresponds to the non-resolved Al 2*p* states from the Cu–Al alloy.[24] Al 2*p* state of the reference aluminum oxide appears at 75.0 eV.[24] In the case of the nanowires, new state appears at 78.8 eV showing again a charge-induced shift of the peak of oxidized aluminum by 3.8 eV, approximately. However, it is overlapped by more intense Cu 3*p* feature.

To understand better the nanowire structure, X-ray diffraction (XRD) analysis was performed. Figure 7 shows the XRD pattern in the 2Θ range from 20 to 70° that was identified as the reflections of monoclinic θ-Al_2O_3 (JCPDS # 86-1410). The mean crystallite size of θ-Al_2O_3 was estimated by using the Sherrer's formula[25] (crystallite size = 0.9λ/B cos θ, where λ = 1.54056 Å, B = FWHM in radians, and θ = the Bragg angle). The (202) and (111) reflection peaks were applied. The size dimensions were 55–65 nm.

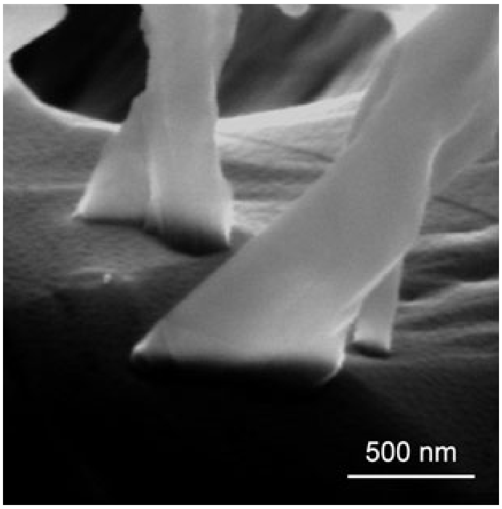

Fig. 5. Side view of wire bottom terminations. The image was acquired in secondary-electron mode (SE).

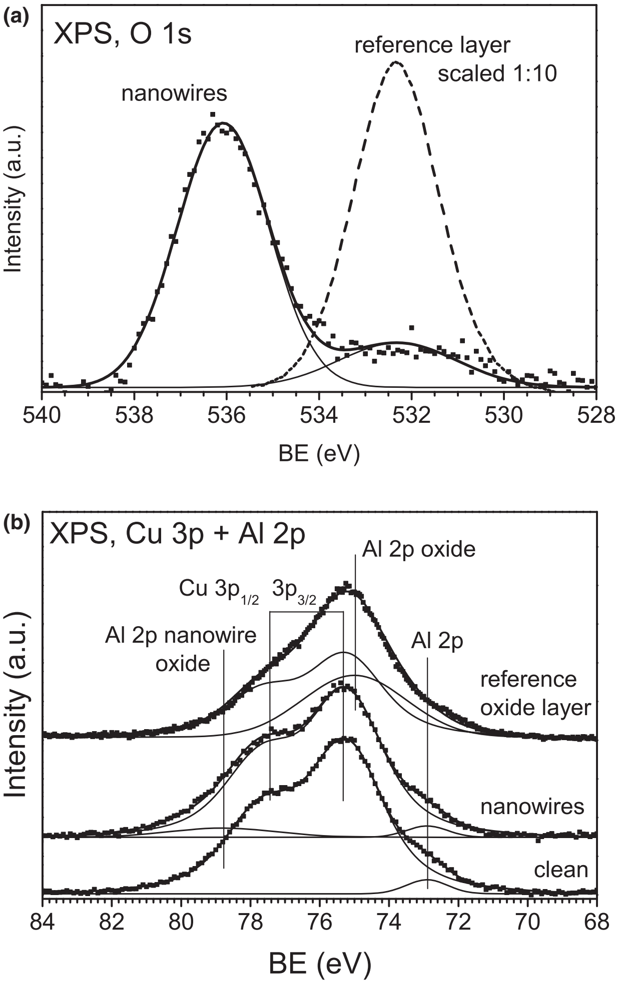

Fig. 6. XPS spectra of the nanowires and the reference alumina layer covering the Cu–9 at.%Al(111) surface: O 1*s* (a), Cu 3*p* + Al 2*p* (b).

The SEM, EDX, XPS, and XRD experiments showed that alumina nanowires can be formed by heating the Cu–9 at.%

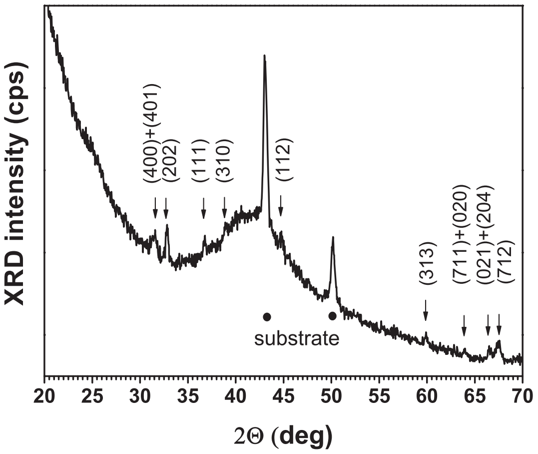

Fig. 7. XRD pattern of the alumina nanowires.

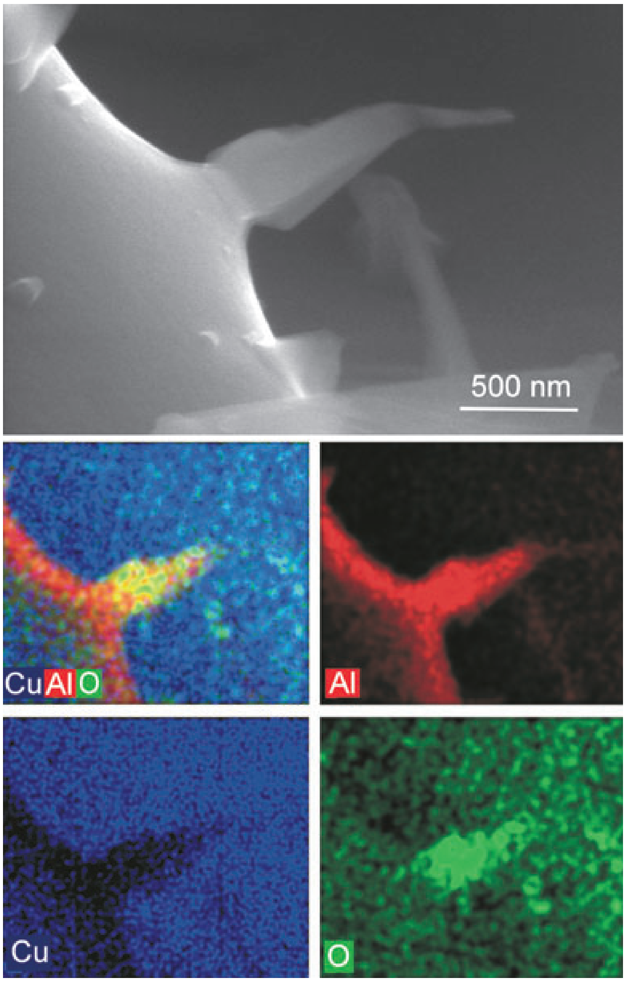

Fig. 8. Side view and EDX element maps of the nanowire base formed on the Cu–9 at.%Al(111) surface point to aluminum segregation in the surface region. The SEM image was acquired in secondary-electron mode (SE). In the EDX maps, Al, O, Cu atoms are represented by red, green, blue colors, respectively.

Al(111) single-crystal in low pressure of oxygen. This process is completely different from usual preparation of nanowires from saturated vapor phase. The process of nanowires' growth is facilitated by a diffusion of aluminum atoms from the bulk toward the surface of the Cu–9 at.%Al(111) substrate, which is known from the thin alumina film growth,[17,24,26] and subsequent diffusion of Al atoms on the hot surface. The difference between growth of continuous films and nanowires is in substrate annealing temperature. Higher temperature assures higher aluminum atom mobility and lower sticking probability of oxygen at the surface,[27,28] i.e. the conditions less favoring the aluminum oxide thin film formation. It results probably in formation of larger aluminum nuclei, which are oxidized with higher probability than single Al atoms interacting with the Cu surface. The hypothesis is supported by Fig. 8 where a SEM side view and element maps of aluminum rich surface region together with nanowire base formation are presented. It is likely that Al atoms are diffusing from Al rich bottom over the nanowire surface toward its end where Al is oxidized due to higher impinging flux of oxygen because of higher accessibility of a small 3-dimensional structure to adsorption from the gas phase. This process results in formation of Al gradient favoring subsequent diffusion of Al atoms from bottom up to the nanowire termination.

IV. Conclusion

In previous studies the formation of ultra-thin monocrystalline alumina layer with the perfect flatness on single crystal Cu–9 at.%Al(111) surface in low pressure of oxygen was reported. In this work we present for the first time a low pressure growth of aluminum oxide nanowires from the Al-containing alloy Cu–9 at.%Al(111). The segregated Al atoms diffusing on the surface form alumina nanostructures at higher annealing temperature compared to the condition of the alumina film preparation. At higher temperature, high mobility of Al atoms and low sticking probability of oxygen result in growth conditions which are not more favored to growth of continuous alumina films. The increase of annealing temperature leads also to changes in alumina crystallographic structure. It clearly shows that a variety of alumina forms can be prepared controlling the annealing time and the substrate temperature: from the continuous well-ordered film to the nanowires.

References

[1] S. A. Chambers, "Epitaxial Growth and Properties of Thin Film Oxides," *Surf. Sci. Rep.*, **39** [5–6] 105–80 (2000).

[2] C. Cibert, H. Hidalgo, C. Champeaux, P. Tristant, C. Tixier, J. Desmaison, and A. Catherinot, "Properties of Aluminum Oxide Thin Film Deposited by Pulsed Laser Deposition and Plasma Enhanced Chemical Vapor Deposition," *Thin Solid Films*, **516** [6] 1290–6 (2008).

[3] K. Koski, J. Hölsä, and P. Juliet, "Properties of Aluminium Oxide Thin Films Deposited by Reactive Magnetron Sputtering," *Thin Solid Films*, **339** [1–2] 240–8 (1999).

[4] X. J. Xu, G. T. Fei, L. Q. Zhu, and X. W. Wang, "A Facile Approach to the Formation of the Alumina Nanostructures from Anodic Alumina Membranes," *Mater. Lett.*, **60** [19] 2331–4 (2006).

[5] J.-H. Zhou, J.-P. He, G.-W. Zhao, C.-X. Zhang, J.-S. Zhao, and H.-P. Hu, "Alumina Nanostructures Prepared by Two-Step Anodization Process," *Trans. Nonferrous Met. Soc. China*, **17** [1] 82–6 (2007).

[6] J. K. Han, J. Kim, Y. C. Choi, K.-S. Chang, J. Lee, H. J. Youn, and S. D. Bu, "Structure of Alumina Nanowires Synthesized by Chemical Etching of Anodic Alumina Membrane," *Physica E*, **36** [2] 140–6 (2007).

[7] X. Zhang, Y. Ge, S.-P. Hannula, E. Levänen, and T. Mäntylä, "Process Study on the Formation of Nanocrystalline α-Alumina with Novel Morphology at 1000°C," *J. Mat. Chem.*, **19** [13] 1915–22 (2009).

[8] A. Boumaza, L. Favaro, J. Lédion, G. Sattonnay, J. B. Brubach, P. Berthet, A. M. Huntz, P. Roy, and R. Tétot, "Transition Alumina Phases Induced by Heat Treatment of Boehmite: An X-Ray Diffraction and Infrared Spectroscopy Study," *J. Solid State Chem.*, **182** [5] 1171–6 (2009).

[9] Z. Gan, G. Ning, Y. Lin, and Y. Cong, "Morphological Control of Mesoporous Alumina Nanostructures via Template-Free Solvothermal Synthesis," *Mater. Lett.*, **61** [17] 3758–61 (2007).

[10] X. Liu, Z. Wu, T. Peng, P. Cai, H. Lv, and W. Lian, "Fabrication of Alumina Nanofibers by Precipitation Reaction Combined with Heterogeneous Azeotropic Distillation Process," *Mater. Res. Bull.*, **44** [1] 160–7 (2009).

[11] S. Wang, M. Shao, L. Lu, H. Wang, H. Gao, and J. Wang, "Silicon Monoxide Assisted Way to Alpha-Alumina Nanostructures and Their Photoluminescence," *Mater. Chem. Phys.*, **112** [1] 230–3 (2008).

[12] R. M. Zaeger, H. Kuhlenbeck, H. J. Freund, M. Wuttig, W. Hoffman, R. Franchy, and H. Ivách, "Formation of a Well-Ordered Aluminium Oxide Overlayer by Oxidation of NiAl(110)," *Surf. Sci.*, **259** [3] 235–52 (1991).

[13]P. Gassmann, R. Francky, and H. Ibach, “Investigations on Phase Transitions Within Thin Al2O3 Layers on NiAl(001) – HREELS on Aluminum Oxide Films,” *Surf. Sci.*, **319** [1–2] 95–109 (1994).

[14]M. Yoshitake, S. Bera, and Y. Yamauchi, “AES and LEED Study of Well-Ordered Oxide Film Grown on Cu-9at.%Al(111),” *Surf. Interface Anal.*, **35** [10] 824–8 (2003).

[15]G. Kresse, M. Schmidt, E. Napetschnig, M. Shishkin, L. Köhler, and P. Varga, “Structure of the Ultrathin Aluminum Oxide Film on NiAl(110),” *Science*, **308** [5727] 1440–2 (2005).

[16]M. F. Luo, J. Y. Huang, C. I. Chiang, G. R. Hu, C. C. Wang, C.T. Wang, and C. W. Lin, “Aligning One-Dimensional Arrays of Nanoclusters on a Thin Film of Al_2O_3 Grown on Vicinal NiAl Surfaces,” *Surf. Sci.*, **603** [3] 558–65 (2009).

[17]M. Yoshitake, S. Bera, Y. Yamauchi, and W. Song, “Oxygen Adsorption on Cu-9at.%Al(111) Studied by Low Energy Electron Diffraction and Auger Electron Spectroscopy,” *J. Vac. Sci. Technol. A*, **21** [4] 1290–3 (2003).

[18]Y. Yamauchi, M. Yoshitake, and W. Song, “Morphology and Thickness of Ultra-Thin Epitaxial Al_2O_3 Film on Cu-9%Al(111),” *Jpn. J. Appl. Phys.*, **42** [7B] 4721–4 (2003).

[19]Y. Yamauchi, M. Yoshitake, and W. Song, “Surface Study and Thickness Control of Thin Al_2O_3 Film on Cu-9at.%Al(111) Single Crystal,” *Appl. Surf. Sci.*, **237** [1–4] 363–8 (2004).

[20]E. Napetschnig, M. Schmidt, and P. Varga, “Ultrathin Alumina Film on Cu-9at%Al(111),” *Surf. Sci.*, **602** [10] 1750–6 (2008).

[21]S. Nemšák, M. Yoshitake, and K. Mašek, “Ultra-Thin Oxide Layer Formation on Cu-9at.%Al(111) Surface and Pd Growth Studied Using Reflection High Energy Electron Diffraction and Auger Elektron Spectroscopy,” *Surf. Sci.*, **600** [18] 4357–60 (2006).

[22]R. F. Egerton, *Physical Principles of Electron Microscopy*. Springer, Edmonton, Canada, 2007.

[23]V. Crist, *Handbook of Monochromatic XPS Spectra*. John Wiley & Sons Ltd, Chichester, England, 2000.

[24]M. Yoshitake, W. Song, J. Libra, K. Mašek, F. Šutara, V. Matolín, and K. C. Prince, “Interface Termination and Band Alignment of Epitaxially Grown Alumina Films on Cu–Al Alloy,” *J. Appl. Phys.*, **103** [3] 33707 (2008).

[25]B. D. Cullity, *Elements of X-Ray Diffraction*. Addison-Wesley, London, 1978.

[26]M. Yoshitake, I. Karas, J. Houfek, S. Madeswaran, W. Song, and V. Matolín, “Position of Segregated Al Atoms and the Work Function: Experimental Low Energy Electron Diffraction Intensity Analysis and First-Principles Calculation of the (√3x√3)R30° Superlattice Phase on the (111) Surface of a Cu-9at.%Al Alloy,” *J. Vac. Sci. Technol. A*, **28** [1] 152–8 (2010).

[27]F. Wiame, V. Maurice, and P. Marcus, “Initial Stages of Oxidation of Cu (111),” *Surf. Sci.*, **601** [5] 1193–204 (2007).

[28]V. Zhukov, I. Popova, and J. T. Yates Jr, “Initial Stages of Al(111) Oxidation with Oxygen-Temperature Dependence of the Integral Reactive Sticking Coefficient,” *Surf. Sci.*, **441** [2-3] 251–64 (1999). ☐